Seismic velocity change in sandstone during CO_2 injection

Marte Gutierrez[1,*], *Daisuke* Katsuki[2], and *Abdulhadi* Almrabat[1]

[1]Civil and Environmental Engineering, Colorado School of Mines, Golden, CO 80401, USA
[2]Petroleum Engineering, Colorado School of Mines, Golden, CO 80401, USA

Abstract. This paper presents analytical and experimental studies of the effects of supercritical CO_2 injection on the seismic velocity of sandstone initially saturated with saline water. The analytical model is based on poroelasticity theory, particularly the application of the Biot-Gassmann substitution theory in the modeling of the acoustic velocity of porous rocks containing two-phase immiscible fluids. The experimental study used a high pressure and high temperature triaxial cell to clarify the seismic response of samples of Berea sandstone to supercritical CO2 injection under deep saline aquifer conditions. Measured ultrasonic wave velocity changes during CO2 injection in the sandstone sample showed the effects of pore fluid distribution in the seismic velocity of porous rocks. CO2 injection was shown to decrease the P-wave velocity with increasing CO2 saturation whereas the S-wave velocity was almost constant. The results confirm that the Biot-Gassmann theory can be used to model the changes in the acoustic P-wave velocity of sandstone containing different mixtures of supercritical CO2 and saline water provided the distribution of the two fluids in the sandstone pore space is accounted for in the calculation of the pore fluid bulk modulus.

1 Introduction

There is now undisputable evidence that anthropogenic release of carbon dioxide (CO_2) in the atmosphere has been the main cause of global climate change [1]. One major solution to reduce the further release of CO_2 in the atmosphere from human activities is geological sequestration (GS), whereby carbon dioxide (CO_2) is injected and permanently stored in underground geological formations particularly saline aquifers. To be economically feasible, CO_2 needs to displace in situ saline water efficiently. Injection of CO_2 is carried out in the form of a supercritical fluid as a result of high in situ fluid pressure and temperature. This is advantageous in terms of injectivity because supercritical CO_2 (referred to as $scCO_2$ in this paper) is less viscous than liquid CO_2 and denser than CO_2 vapor.

One of the main technical issues in CO_2 geological sequestration is the prediction and monitoring of the flow, transport and prolonged stability of CO_2 in deep saline formations. Development of field monitoring techniques for CO_2 migration is also essential for the safe and reliable operations of CO_2 sequestration. Field monitoring is crucial to determine injected CO_2 movement, volumes and locations in the sequestration reservoir. Direct monitoring techniques use observation wells and tracers to observe CO_2 migration in reservoirs. However, drilling observation wells is expensive, time consuming, provides only limited data which may not fully represent in situ conditions, and has the risk of deteriorating the sealing capacity of the cap rock.

Indirect geophysical methods such as seismic and electric resistivity surveys can be used for economical, large-scale field underground fluid monitoring. Time-lapsed seismic survey mapping can provide spatial distribution of seismic wave velocity which can be correlated with CO_2 migration and volumes in a storage reservoir with time. The acoustic velocity response of rock media filled with fluids is primarily a function of rock mass elasticity, porosity, and pore fluid bulk modulus. These components, related to acoustic velocity, are affected by temperature, rock mass effective stresses, fluid pressure, and pore fluid composition (saturation). Previous studies [2,3] have shown that the acoustic velocity response of sandstone cores changes with the relative volumes of water/CO_2 in the pore space. The change in acoustic velocity is a result of the change in the bulk modulus of the pore fluid as $scCO_2$ displaces saline water during the injection process. However, the evaluation of the bulk modulus of mixture of multiphase fluid is still a challenge. A major reason is that the bulk modulus of a fluid mixture should also depend on the degree of uniformity of the fluid mixture in the rock pore space [4,5].

This paper presents mathematical and experimental investigations of the effects of supercritical CO_2 injection on the seismic velocity of sandstone initially saturated with saline water. The mathematical model is based on application of the Biot-Gassmann poroelasticity theory [6,7] in the modelling of the acoustic velocity of porous rocks containing two-phase immiscible pore fluids. The focus of the mathematical modelling is on how the Biot-Gassmann theory can be modified to account for the distribution of two-phase fluids, particularly in terms of layering and non-uniformity in the $scCO_2$ displacement front, in addition to their relative

* Corresponding author: mgutierr@mines.edu

volumes, in the pore space of sandstone. The experimental study uses a laboratory testing system to clarify the acoustic response of rocks to supercritical CO_2 injection under deep saline aquifer conditions. The main component of the system is a high pressure and high temperature (HPHT) triaxial cell that allows for injection of CO_2 in core samples of sandstone initially saturated with saline water. High pressure precision syringe pumps for back pressure and injection fluid pressure control, a hydraulic pump for cell pressure control, and a temperature control system allow for the injection of CO_2 at supercritical conditions. The end caps of the core holder are equipped with piezoelectric transducers to characterize ultrasonic wave velocity response of the rock core sample.

2 Biot-Gassmann Theory

Gassmann's substitution theory [7] is the most widely used equation to describe the effects of the bulk modulus of the pore fluid on the seismic velocity of deformable porous media. The original derivation of Gassmann's equation is very involved and complicated. Here, it is shown that the equation can be derived very elegantly and succinctly using Biot's poroelastic equations. The coupled poroelastic equations, which were first derived by [6], provide a rigorous mathematical treatment of fluid flow in deformable porous media, where fluid flow affects mechanical response and vice versa, and fluid flow field cannot be analyzed separately from the mechanical response except under simple boundary conditions. (Notes: (a) tensorial notation is used and repeated indices imply summation, (b) a dot over a symbol indicates differentiation with respect to time, and (c) all stresses are total). Biot's theory couples the poroelastic stress-strain relation for fluid-saturated porous materials:

$$\dot{\sigma}_{ij} = K\dot{\varepsilon}_v\delta_{ij} + 2G\dot{e}_{ij} - \alpha\delta_{ij}\dot{p} \tag{1}$$

with the poroelastic fluid diffusion equation that quantifies fluid pressure changes in the same material (assuming single phase fluid flow and isotropic permeability):

$$\nabla\cdot\left(\nabla\frac{k}{\mu}p\right) = \alpha\dot{\varepsilon}_v + \left(\frac{\phi}{K_f} + \frac{\alpha-\phi}{K_s}\right)\dot{p} + \dot{q} \tag{2}$$

In the above equations $\nabla = \partial/\partial x_i$, $\dot{\sigma}_{ij}$ =stress rate tensor, $\dot{\varepsilon}_v = \dot{\varepsilon}_{kk} = \dot{\varepsilon}_{ij}\delta_{ij}$ =volumetric strain rate tensor, $\dot{e}_{ij} = \dot{\varepsilon}_{ij} - \delta_{ij}\dot{\varepsilon}_v/3$ =deviatoric strain rate tensor, $\dot{\varepsilon}_{ij}$ =strain rate tensor, $\dot{p}$ =pore pressure rate, k = permeability, μ =fluid viscosity, $\dot{q}$ =fluid source or sink, K and G =elastic bulk and shear moduli of the porous medium, respectively, δ_{ij} =Kronecker delta, K_f and K_s = bulk moduli of the pore fluid and the solid grains of the porous medium, respectively, ϕ =porosity, and α =Biot's poroelastic constant defined as:

$$\alpha = 1 - \frac{K}{K_s} \tag{3}$$

In Eq. (2), single phase fluid flow and isotropic permeability were assumed. As will be shown below, permeability disappears in the derivation of the Biot-Gassmann equation. For this reason and by defining the pore pressure p as the average fluid pressure, the Biot-Gassmann equation that will be derived below based on the Eqs. (1) and (2) can also be used for two phase fluid flow. Note that Eq. (1) differs from conventional elasticity in that poroelastic deformation of the solid grains due to pore pressure changes is included in the total deformation of the porous medium. Eq. (2) also differs from conventional fluid diffusion equation in that it accounts for poroelastic deformation in the fluid flow in the porous medium.

Under undrained conditions, two conditions are achieved: (1) $(\nabla kp/\mu) = 0$ (i.e., no fluid gradients or Darcy fluid flow), and (2) $\dot{q} = 0$ (i.e., no fluid sink or source). Substituting these two conditions in Eq. (2) and solving for $\dot{p}$ gives:

$$\dot{p} = -\frac{\alpha\dot{\varepsilon}_v}{\left(\frac{\phi}{K_f} + \frac{\alpha-\phi}{K_s}\right)} \tag{4}$$

Since the shear modulus G is independent of pore fluid composition and is the same for both drained and undrained conditions [8], Eq. (1) can be split into deviatoric and volumetric components:

$$\dot{s}_{ij} = 2G\dot{e}_{ij} \text{ and } \dot{\sigma}_m = K\dot{\varepsilon}_v - \alpha\dot{p} \tag{5}$$

where $\dot{\sigma}_m = \dot{\sigma}_{kk}/3 = \dot{\sigma}_{ij}\delta_{ij}/3 =$ mean stress rate, and $\dot{s}_{ij} = \dot{\sigma}_{ij} - \delta_{ij}\dot{\sigma}_m$ =deviatoric stress rate tensor. The validity of uncoupling the deviatoric and volumetric elastic response of fluid saturated porous media is investigated experimentally below. Substituting Eq. (4) in Eq. (5) yields:

$$\dot{\sigma}_m = K\dot{\varepsilon}_v + \frac{\alpha^2\dot{\varepsilon}_v}{\left(\frac{\phi}{K_f} + \frac{\alpha-\phi}{K_s}\right)} \tag{6}$$

Dividing throughout by $\dot{\varepsilon}_v$ yields the undrained bulk modulus of a fluid-saturated porous rock $K_u = \dot{\sigma}_m/\dot{\varepsilon}_v$ as:

$$K_u = K + \frac{\alpha^2}{\left(\frac{\phi}{K_f} + \frac{\alpha-\phi}{K_s}\right)} \tag{7}$$

Eq. (7) was first derived by [7], however, as shown above this equation can also be derived from the more general and earlier Biot's poroelasticity theory. Thus, it is only proper to call Eq. (7) as the Biot-Gassmann equation. Eq. (7) gives the undrained bulk modulus of fluid-saturated porous material as function of the drained or dry bulk modulus of the same material, the porosity, Biot's poroelastic constant, and bulk moduli of the pore fluid and the solid grains of the porous medium. The different parameters in Eq. (7) are all constants for a rock specimen under the same effective stress and porosity except for the pore fluid bulk modulus which can change with fluid composition. It is important to

note that the second term of the right-hand side of Eq. (7) represents the effect of pore fluid content on the undrained bulk modulus K_u.

3 Laboratory Testing Equipment

The effects of injection of $scCO_2$ in the seismic velocity of porous rock were studied using a high-pressure and high temperature (HPHT) triaxial cell. A schematic diagram of the complete system is shown in Fig. 1. The triaxial core holder has a maximum working confining pressure capacity of 70 MPa, two precision syringe pumps that control the back pressure and injection pressure, a dome-loaded back pressure regulator, a hydraulic pump for regulating cell pressure, and a differential pressure transducer. The sample having diameter of 38 mm the length up to 76 mm is enclosed in a Viton sleeve. Both ends of the core sample are in contact with high permeability porous metal filter discs in order to homogenize the fluid flow. Two movable pistons controlled by hydraulic pressure can induce axial stress different from the confining stress. One of the syringe pumps transmits a mixture of saline water and $scCO_2$ into the rock core sample at very accurate flow rates. Another syringe pump acts as the back-pressure regulator with set-point pressure. The pressure and volume change of fluids in the syringe pumps are monitored and acquired in a personal computer communicating with the pumps. The back-pressure regulator is equipped with a polyimide film diaphragm providing accurate regulation of outlet pressures. Saline water produced from the end face of rock core sample during $scCO_2$ injection is accumulated in a vessel placed on an accurate electronic balance. The mass data of saline water accumulated is acquired by using a computer via serial communication.

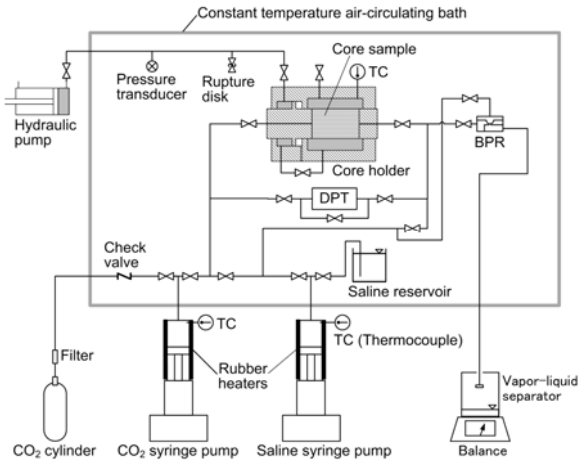

Fig. 1. Schematic diagram of the testing system.

The end caps of the core holder are equipped with piezoelectric transducers for seismic compressional and shear wave velocity measurements. Fig. 2 shows a schematic of the arrangement of piezoelectric transducers which are 1x4x6 mm^3 in size. Triads of shear wave transducers shake one of the end caps in two individual orthogonal directions. In the center of the cap is a compressional wave transducer.

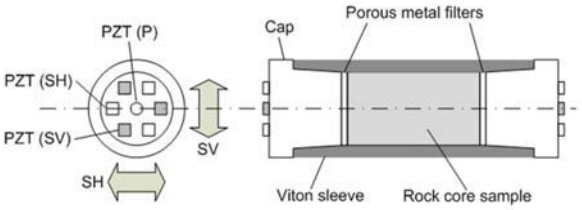

Fig. 2. Arrangement and polarization of piezoelectric transducers for seismic wave velocity measurement. Arrows indicate the direction of oscillation of two different shear waves (horizontal "SH" and vertical "SV"), and "P" denotes compression wave.

The natural frequencies of the transducers range from 0.25 to 1 MHz. The transducers are excited by using a square wave pulser/receiver capable of providing square pulses whose voltages are selectable between 100 and 400 V in increments of 100 V. The typical rise time of pulse is less than 1.0×10^{-8} s which is considered to be in the quasi-static range. The maximum bandwidth and typical noise level of receiver are from 1 kHz to 35 MHz and 70 μV peak to peak, respectively. The seismic waveforms are converted into digital signals by using a digital oscilloscope having 100 MHz of bandwidth and 1×10^{9} s^{-1} of real time sample rate. The minimum time base and the vertical resolution of the oscilloscope are 2×10^{-9} s/div and 8 bits. The waveform data are acquired by using a personal computer communicating with the oscilloscope. Each waveform acquired is the average of 16 waveforms. The resultant minimum time interval of waveform acquisition in the personal computer is 6 s.

4 Test Materials and Procedures

The study of the effects of $scCO_2$ injection in the seismic velocity of porous rock initially saturated with saline water was conducted using Berea sandstone, which is a well-known and widely used test material in the study of the rock mechanical and fluid flow behavior of sedimentary rocks. Cylindrical rock samples used for the experimental works are cored from a block of Berea sandstone. Both ends of the core samples are grinded to ensure that sample ends are parallel within required tolerances. The Berea sandstone used has a dry density of 2.2 g/cm^3, 17% porosity and permeability of 20-30 mD. Carbon dioxide having 99.9999% of purity is used to prepare the $scCO_2$. Saline water used is a mixture of distilled water and sodium chloride at 3.4% of salinity.

The procedure for the $scCO_2$ injection tests is described below. A core sample dried at 100°C is placed inside the core holder then saturated with distilled water under vacuum by allowing the sample to imbibe distilled water. The confining axial and lateral stresses are isotropically increased up to 12 MPa. The pore pressure P_{pore} is simultaneously raised to 10 MPa by keeping the effective stress less than 2 MPa. The core sample is consolidated at desired effective stress at a pore pressure of P_{pore} = 10 MPa and a temperature of T = 40°C to

ensure that the injected CO_2 is kept in supercritical condition. Distilled water filling the pore space is displaced with saline water saturated with $scCO_2$ at P_{pore} = 10 MPa and T = 40°C. The total volume of saline water injected is more than ten times of the pore volume of core sample. Supercritical CO_2 saturated with saline water is injected into core sample at a constant rate at the prescribed conditions. The injection rates q_{inj} of $scCO_2$ during the relative permeability characterization and ultrasonic wave velocity measurement are 2.0 and 0.20 cm^3/min, respectively. The pressure values used in the paper are gage pressures.

5 Test Results and Discussions

Fig. 3 shows the injection pressure and saline water production behavior observed during CO_2 injection at a rate of 0.2 cm^3/min. The injection pressure is maintained at 10.00±0.05 MPa through displacement. The production behavior of saline water indicates that CO_2 reaches a maximum saturation of 0.25 at the end point of displacement.

Fig. 4 shows some of the waveforms of P-wave acquired during the CO_2 injection. The values in the Figures indicate the average CO_2 saturation of the core sample when a P-wave velocity is measured. The arrival time of each wave has been determined at the first negative rise in the waveform. The arrival time changed significantly from 36.0 to 36.6 ms and subsequently to 37.2 ms as the CO_2 saturation increased from 0 to 0.151 and to 0.214.

The shear waveforms acquired during CO_2 injection are shown in Fig. **5**. The arrival times are 64.4, 64.4, and 64.0 ms corresponding to the average CO_2 saturation values of 0.0, 0.137 and 0.228, respectively. The arrival time was determined at the first negative rise in the waveform. The dependency of shear wave velocity on $scCO_2$ saturation seems to be very different to that of the P-wave, i.e., the S-wave velocity increases slightly with increasing the CO_2 saturation, and is almost insensitive to the $scCO_2$ saturation.

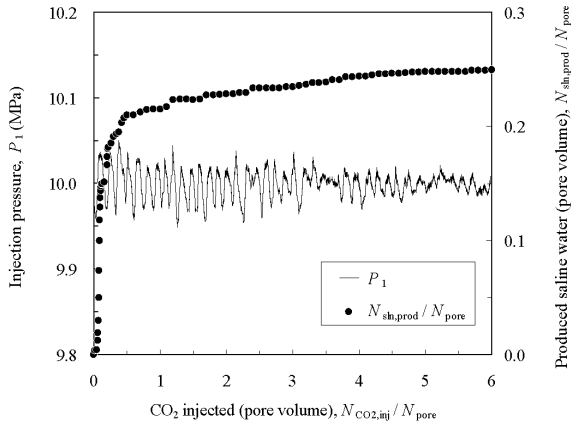

Fig. 3. Injection pressure and production behavior during CO_2 injection at 0.2 cm^3/min into Berea sandstone core sample presaturated with saline water.

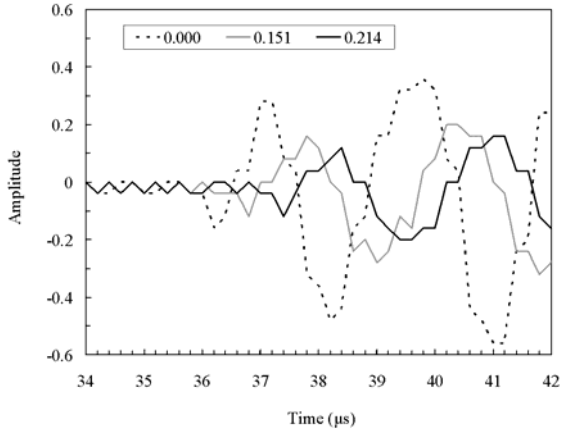

Fig. 4. Compression waveform change depending on CO_2 saturation observed during CO_2 injection into Berea sandstone core sample pre-saturated with saline water.

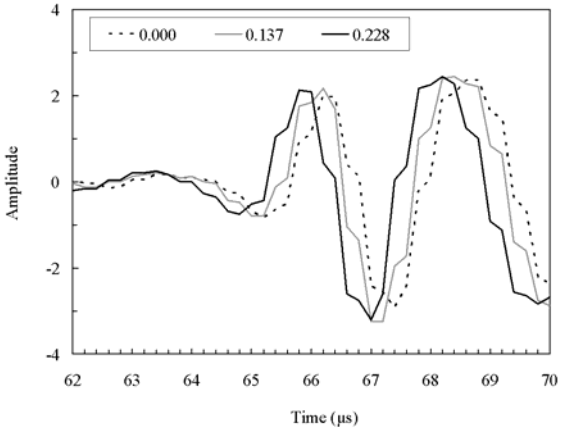

Fig. 5. Change of shear waveforms during CO_2 injection at 0.2 cm^3/min into Berea sandstone core sample pre-saturated with saline water.

The CO_2 saturation dependency of the bulk and shear moduli of Berea sandstone is summarized in Fig. **7**. The bulk and shear moduli, K and G were calculated from

$$K = \rho\left(V_p^2 - \frac{4}{3}V_s^2\right) \quad (8)$$

$$G = \rho V_s^2 \quad (9)$$

where V_p and V_s are the compressional and shear wave velocities, and ρ is the density of porous medium. The bulk density of porous rock filled with saline water and CO_2 is calculated from

$$\rho = \rho_{dry} + \phi\left[S_{CO2}\rho_{CO2} + (1 - S_{CO2})\rho_{sln}\right] \quad (10)$$

where ρ_{dry}, ρ_{CO2}, and ρ_{sln} are the bulk densities of the dry rock, CO_2, and saline water, and ϕ is the porosity of the rock sample. In Fig. **6** and Eq. (10), S_{CO2} is the $scCO_2$ saturation which is defined as the volume of supercritical CO_2 in the voids divided by the volume of the voids. The error bars indicate the uncertainty in the determination of the P-wave arrival time, which was less distinct than that of S-wave. As can be seen in Fig. **6**, the bulk modulus decreased from 17.5 GPa to 13.3 GPa during the

displacement of saline water by $scCO_2$. The pore fluid bulk modulus, and correspondingly the rock undrained bulk modulus K_u, decreased with increasing S_{CO2} because the $scCO_2$ bulk modulus is lower than saline bulk modulus. Note that most of the change in the bulk modulus occurred for S_{CO2} <0.25. This is because the irreducible saline water saturation for the tested sample is about 75%. In contrast to the bulk modulus, Fig. **6** shows that the shear modulus is nearly constant during the increase in $scCO_2$ saturation from 0 to 0.25. This confirms the assumption used in Eq. (5) to uncouple the elastic volumetric and deviatoric responses in a poroelastic medium.

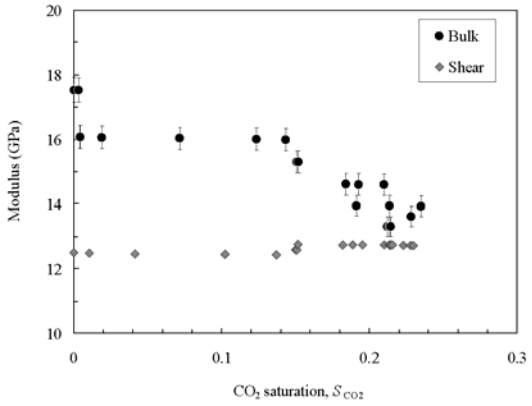

Fig. 6. CO_2 saturation dependencies of bulk and shear moduli of Berea sandstone core sample.

To calculate the undrained bulk modulus K_u in Eq. (7), it is necessary to determine the pore fluid bulk modulus K_f. Two widely used equations to calculate the bulk modulus of mixtures of two phase immiscible fluids are: (1) the serial law, and (2) the Wood's (1941) parallel law [9]. For a mixture of saline water and $scCO_2$, the serial law is given as:

$$K_f = S_{CO2}K_{CO2} + (1 - S_{CO2})K_{sln} \tag{11}$$

and Wood's parallel law as:

$$\frac{1}{K_f} = \frac{S_{CO2}}{K_{CO2}} + \frac{1 - S_{CO2}}{K_{sln}} \tag{12}$$

where K_{CO2} is the bulk modulus of $scCO_2$ and K_{sln} is the bulk modulus of saline water. The serial law is applicable to the case where the two immiscible fluids are segregated perpendicular to the wave propagation direction (Fig. **7a**), and the parallel law is applicable to the case where the two immiscible fluids are segregated parallel to the wave propagation direction (Fig. **7b**).

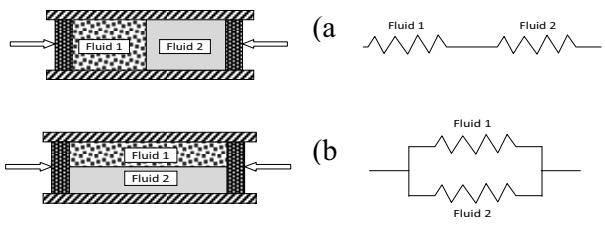

Fig. 7. Illustration of (a) serial and (b) parallel distributions of two-phase fluids in respect to longitudinal direction.

The dependency of V_p on S_{CO2} of the tested Berea sandstone is shown in Fig. **8**. The S_{CO2}-dependent V_p is calculated and predicted from K_u (Eq. 7), with K_f determined from either Eq. (10) or Eq. (1), and G as:

$$V_p = \sqrt{\frac{1}{\rho}\left(K_u + \frac{4}{3}G\right)} \tag{13}$$

As can be seen, V_p decreases from 3.86 km/s to approximately 3.65 km/s as S_{CO2} increases from 0 to 0.25. The V_p vs. S_{CO2} relationships calculated from the Biot-Gassmann equation in combination with the bulk modulus values from the serial and parallel distributions (Eqs. 10 and 11) are also shown in the figure. The pressure and temperature fluid bulk modulus values for $scCO_2$ were obtained from [2] and [10]. The Biot-Gassmann equation in combination with serial law (Eq. 10) predicts rapid decrease of V_p with values much lower than experimental data, while the Biot-Gassmann equation in combination with parallel law (Eq. 11) predicts a slower decrease in V_p with increasing $scCO_2$ saturation than experimental data.

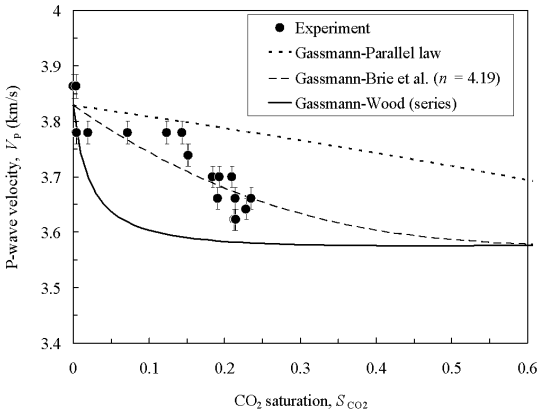

Fig. 8. CO_2 content dependency of compressional wave velocity during CO_2 injection into Berea sandstone pre-saturated with saline water**.**

The results shown in Fig. 8 indicate that the two-phase fluids are potentially distributed neither in parallel nor serial fashion in the test specimen, although these distributions correspond to the lower and upper bound values, respectively, of the V_p vs. S_{CO2} relationship in sandstone. X-ray CT (Computed Tomography) imaging of $scCO_2$ injection in Berea sandstone shows that the pore fluid distribution is more complicated than the ideal parallel or serial distributions and is dependent on the pore structure and the relative mobilities of the two fluids (Shi et al., 2011). A much improved empirical equation to estimate the fluid bulk modulus of mixtures two-phase fluids and account for their mixing is the equation proposed by Brie et al. [4]:

$$K_f = S_{\text{sln}}^n K_{\text{sln}} + \left(1 - S_{\text{sln}}^n\right) K_{\text{CO2}} \quad (14)$$

where $S_{\text{sln}} = 1 - S_{CO2}$ =saline water saturation and n=empirical parameter. Note than n=1 corresponds to the serial fluid distribution. As the value of n increases, the effect of the lower bulk modulus of CO_2 phase becomes predominant at lower CO_2 saturations. The value of n determined by fitting the resulting V_p vs. S_{CO2} curve to the experimental data is 4.19 with R^2-value of 0.85. The data-fitted V_p vs. S_{CO2} curve corresponding to the combined equation of Biot-Gassmann (Eq. 7) and Brie (Eq. 14) is shown in Fig. 8 together with the experimental data. As can be seen, a good agreement is obtained indicating the validity of the combined Biot-Gassmann-Brie equations.

The change in the V_p–S_{CO2} relationship shown in Fig. 8 should correspond to the transitions of the fluid distributions in the core sample. At the very early stage of displacement (S_{CO2} < 0.02), the observed V_p–S_{CO2} relationship has changed along the curve given by the Gassmann-Wood equation. This change can be understood by considering the following displacement process. The injected CO_2 phase is likely to concentrate in the inlet end of core sample at this stage. The rest of pore space should not be invaded by CO_2. The fluids are therefore close to the series distribution to which the Wood's law is applicable.

When S_{CO2} is increased from 0.02 to 0.15, the V_p–S_{CO2} relationship observed has moved close to that given by the Gassmann-parallel law model. This transition means that the fluid distribution is shifting to a layered distribution. This is reasonable because the injected CO_2 can concentrate in the upper part of the horizontally oriented core sample due to buoyancy effect and consequently the saline water and CO_2 phases flow in two distinct layers.

After that, the observed V_p–S_{CO2} relationship gradually moved toward that predicted by the Gassmann-Wood equation. This transition is understandable by considering a process in which the layered fluid distribution is changing gradually to a homogeneous one as the fluid displacement proceeds. More specifically, the volume of the saline water occupying the outlet end of the core sample has now been gradually displaced by CO_2, and CO_2 occupies most of the pore space. The observed V_p remains higher than that predicted by the Gassmann-Wood equation even at the end point of displacement. This suggests that the fluid distribution still has some heterogeneity at the end point of displacement. On the average, the combined Biot-Gassmann-Brie equation with an exponent of 4.19 provides a very good representation of the pore fluid dependent P-wave velocity of Berea sandstone.

6 Conclusions

Ultrasonic wave velocity changes due to CO_2 saturation change were determined using Berea sandstone core sample which was initially saturated with saline water and was subjected to constant CO_2 injection rate. The results showed the effects of pore fluid distribution in determining the effects of multiphase pore fluids on the seismic velocity of porous rocks. Increasing CO_2 saturation affected the P-wave velocity which was observed to decrease whereas the S-wave velocity was almost constant during the CO_2 injection. The results confirm that the Biot-Gassmann theory can be used to model the changes in the acoustic P-wave velocity of sandstone containing different mixtures of supercritical CO_2 and saline water provided the distribution of the two fluids in the sandstone pore space is accounted for in the calculation of the pore fluid bulk modulus. Two-phase fluids distributed parallel and in series in the voids relative to the wave propagation direction correspond to the lower and upper bound values, respectively, of the fluid saturation dependent P-wave velocity of sandstone. The observed relationship between P-wave velocity and CO_2 saturation transitioned from the relation given by the Biot-Gassman-Wood model in the initial injection phase, to the Biot-Gassmann-parallel law model, then back to the Biot-Gassmann-Wood model towards the end of the displacement process. This should correspond to the transition of spatial distribution of saline water and CO_2 in core sample as the displacement of saline water proceeded. The empirical relation of Brie et al. [4] for the bulk modulus of mixtures of two-phase immiscible fluids, in combination with the Biot-Gassmann theory, was found to satisfactorily represent the pore-fluid dependent acoustic P-wave velocity of sandstone.

Financial support provided by the Department of Energy under grant no. DE-FE0000730 is gratefully acknowledged.

References

1. IPCC-Intergovernmental Panel on Climate Change, *Special Report on Carbon Dioxide Capture and Storage*. Chapter 5 (2005).
2. J. K. Kim, J. Xue, T. Matsuoka, "Experimental study on CO2 monitoring and saturation with combined P-wave velocity and resistivity." SPE Journal, SPE 130284 (2010).
3. Q. Shi, Z. Q. Xue, S. Durucan, "Seismic monitoring and modelling of supercritical CO2 injection into a water-saturated sandstone: Interpretation of P-wave velocity data." Intl. J. Greenhouse Gas Control, **1(4)** (2007).
4. A. Brie, F. Pampuri, A. F. Marsala, O. Meazza, "Shear sonic interpretation in gas-bearing sands." Proc. SPE Ann. Tech. Conf. & Exhb., Dallas, Texas (1995).
5. A. L. Endres, R. Knight, "The effects of pore-scale fluid distribution on the physical-properties of partially saturated tight sandstones." J. Appl. Phys. **69(2)** (1991).
6. M. Biot, "General theory of three-dimensional consolidation." J. Appl. Phys. **12** (1941).
7. F. Gassmann, "Über die elastizität poröser medien." Viertel Naturforsch Ges Zürich **96** (1951).
8. J. G. Berryman. Origin of Gassman's equations." Geophysics, **64** (1999).
9. A. B. Wood *A Textbook of Sound* Bell and Sons LTD, London (1941).
10. M. Batzle, Z. J. Wang, "Seismic properties of pore fluids." Geophysics, **57(11)** (1992).